

Lifetime measurements of highly deformed bands in $^{134,135}\text{Nd}$ and ^{131}Ce

C. M. Petrache,^{1,*} R. Wyss,² Zs. Podolyák,^{3,†} D. Bazzacco,¹ G. de Angelis,³ D. de Acuña,³ M. De Poli,³ A. Dewald,⁴
 E. Farnea,³ J. Gableske,⁴ A. Gadea,^{3,‡} S. Lunardi,¹ D. R. Napoli,³ M. N. Rao,^{1,§} C. Rossi Alvarez,¹ T. Scanferla,¹
 C. A. Ur,^{1,*} R. Venturelli,¹ P. von Brentano,⁴ and L. H. Zhu^{1,**}

¹Dipartimento di Fisica and INFN, Sezione di Padova, 35131 Padova, Italy

²Royal Institute of Technology, Physics Department Frescati, S-10405 Stockholm, Sweden

³INFN, Laboratori Nazionali di Legnaro, 35020 Legnaro, Italy

⁴Institut für Kernphysik der Universität zu Köln, Germany

(Received 20 October 1997)

The quadrupole moments of highly deformed bands in $^{134,135}\text{Nd}$ and ^{131}Ce have been determined using the Doppler-shift attenuation method. The obtained Q_0 values show no clear dependence on the number of occupied $\nu i_{13/2}$ intruder orbitals. Cranked shell model calculations indicate that the charge-quadrupole moments of the highly deformed bands decrease with increasing spin. The expected increase in deformation induced by the $\nu i_{13/2}$ orbital in two bands of ^{134}Nd is attenuated by a rotation-induced shrinking effect driving the nucleus towards smaller deformation. [S0556-2813(98)50401-3]

PACS number(s): 21.10.Tg, 21.10.Re, 23.20.Lv, 27.60.+j

The highly deformed (HD) bands observed in the $A=130$ mass region are based on ellipsoidal shapes with approximate axis ratio 3:2 ($\beta_2=0.3-0.4$), which differ from the shapes on which the normal-deformed bands are based ($\beta_2=0.15-0.25$). These elongated shapes are stabilized by the shell gaps in the *static* single-particle energy spectrum, which, in the case of the $A=130$ nuclei, occur at $Z=58$ and $N=72$, $N=6$. The occupancy of the $N=6$ $\nu i_{13/2}$ intruder orbitals is essential for the observation of the HD bands at high spin [1]: due to the strong Coriolis coupling of high- j orbitals, the two signature partners of the $\Omega=1/2$ $\nu i_{13/2}$ orbital cross the $N=72$ gap at quite low rotational frequency and induce *dynamic* shell gaps at $N=73$, $N=74$ [1,2]. Therefore, it is not easy to disentangle between the contribution of the $N=72$ shell gap and that of the intruder orbitals to the stabilization of the highly deformed minimum in the $A=130$ mass region. The dependence of the quadrupole deformation on the number of high- N intruder orbitals is well established in the $A=150$ mass region from the lifetime measurements performed for the superdeformed bands of $^{148,149}\text{Gd}$, ^{152}Dy [3], $^{151,152}\text{Dy}$, ^{151}Tb [4], being understood theoretically by the additivity of the independent contributions from the individual hole or particle orbitals to the doubly magic superdeformed core ^{152}Dy [5]. In the $A=130$ mass region, on the contrary, the absence of a clear dependence of the quadrupole deformation on the number of occupied intruder orbitals has been inferred from the reported equal quadrupole moments for the yrast HD bands of ^{131}Ce

and ^{132}Ce [6], assumed to be based on $\nu i_{13/2}$ and $\nu(i_{13/2})^2$ configurations, respectively. Since cranked shell-model calculations predict a difference in deformation of $\sim 10\%$ between the configurations with one and two $\nu i_{13/2}$ orbitals [7], the conclusion was drawn in Ref. [6] that the shape-driving force of the $\nu i_{13/2}$ orbital is less than expected. However, different quadrupole moments have been reported in the same paper for the yrast and excited HD bands of ^{131}Ce , which involve also one and two $\nu i_{13/2}$ orbitals, respectively.

The present lifetime measurements are intended to study further the shape-polarizing effect of the $\nu i_{13/2}$ intruder orbital, this time in the ^{134}Nd nucleus, where quite a good understanding of the underlying configurations of the HD bands has been acquired [8]. In our previous works on ^{134}Nd , we reported two bands built on the second minimum and two bands which at high spin seem to evolve towards high deformation through the consecutive step-wise occupation of the first and second $\nu i_{13/2}$ orbitals [2,8,9]. The existence in ^{134}Nd of high-spin bands built on configurations with zero, one or two $\nu i_{13/2}$ intruder orbitals over well-defined frequency ranges, makes this nucleus a favorite case to study the deformation-driving effects of the $\nu i_{13/2}$ intruder orbitals. The present experiment was aimed at the determination of the quadrupole moments for several HD bands from the same measurement exploiting the high efficiency of the modern detectors arrays, which enables the simultaneous observation of several HD bands populated in the same reaction. In this way, the systematic uncertainties (associated mainly with the stopping powers, but also with the beam energy, target thickness, etc.) are considerably reduced, allowing the extraction of precise relative quadrupole moments. Measurements of this type have been reported in $^{131,132}\text{Ce}$ [6], $^{132,133}\text{Ce}$ [10], $^{148,149}\text{Gd}$ and ^{152}Dy [3], and $^{151,152}\text{Dy}$ and ^{151}Tb [4].

The highly deformed bands of the $^{134,135}\text{Nd}$ and ^{131}Ce nuclei have been populated via the $^{110}\text{Pd}(^{28}\text{Si},xny\alpha)$ reaction at a beam energy of 132 MeV. The target consisted of 1 mg/cm^2 ^{110}Pd evaporated on a 10 mg/cm^2 thick Au back-

*On leave from Institute of Physics and Nuclear Engineering, Bucharest, Romania.

†On leave from Babeş-Bolyai University, Cluj-Napoca, Romania.

‡On leave from Instituto de Física Corpuscolar, Valencia, Spain.

§On leave from Instituto de Física, Universidade de São Paulo, São Paulo, Brazil.

**On leave from China Institute of Atomic Energy, Beijing, People's Republic of China.

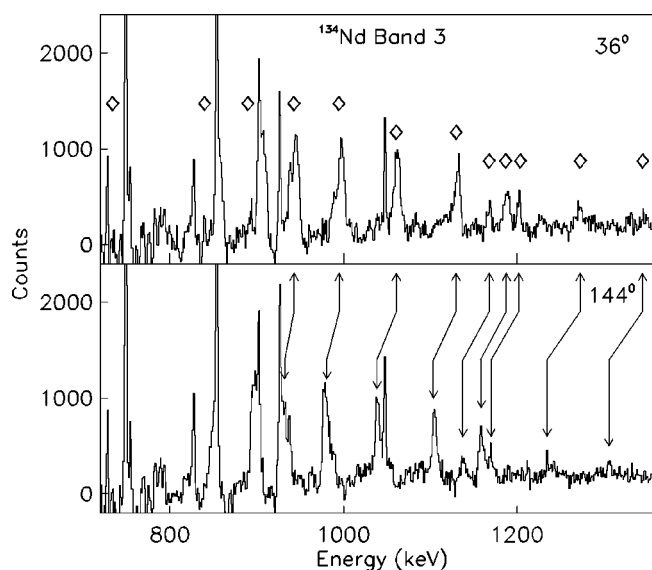


FIG. 1. Spectra for band 3 of ^{134}Nd at 36° and 144° , obtained from combinations of all double gates on the in-band transitions above the 748 keV γ ray. In the upper panel the in-band transitions are marked with diamonds.

ing. The beam was provided by the XTU Tandem accelerator of the Legnaro National Laboratories. The gamma spectrometer (GASP) array with 40 Compton-suppressed HPGe detectors and the 80-element bismuth orthogermanate (BGO) inner ball was used for gamma-ray detection. The Italian Silicon Sphere (ISIS) ball consisting of 40 $\Delta E-E$ Si-telescopes was used for charged particles detection. Events were collected when three or more Ge detectors fired in coincidence with at least four BGO detectors. A total of 1.9×10^9 triple and higher-fold Compton-suppressed events were collected. For every band of interest, the data were sorted off-line in double-gated spectra from all detectors, but projecting only those at definite angles to the beam, namely at 36, 60, 72, 90, 108, 120, 144 deg. The use of the ISIS ball in separating the $4n$ and $\alpha 3n$ reaction channels was essential to obtain accurate centroid shifts for the nearly degenerate peaks in the lower part of the yrast HD bands of ^{134}Nd and ^{131}Ce , respectively. The spectra of the yrast band of ^{134}Nd have been obtained by imposing a veto on α particles, which suppressed the $\alpha 3n$ channel, whereas those of the HD band of ^{131}Ce have been obtained by selecting events in coincidence with α particles. Typical double-gated spectra at forward and backward angles are shown in Fig. 1 for band 3 in ^{134}Nd (see Ref. [8]).

The analysis has been performed using the Doppler shift attenuation method (DSAM) [11]. The fractional Doppler shifts $F(\tau)$, i.e., the ratio between the average recoil velocity at which a state decays and the average initial velocity (v_0), were determined from the γ -ray peak centroids extracted from different angles. The initial velocity of the recoiling Nd nuclei was calculated using the bombarding energy at the midpoint of the ^{110}Pd target and assuming that the evaporated neutrons did not perturb the average speed; a value of $v_0/c=0.0202(2)$ has been found, which is consistent with the Doppler shift of the highest observed transitions in the bands. Note that the fractional shifts of the transitions at the top of the bands do not go to 1 (see Fig. 2 below). This is

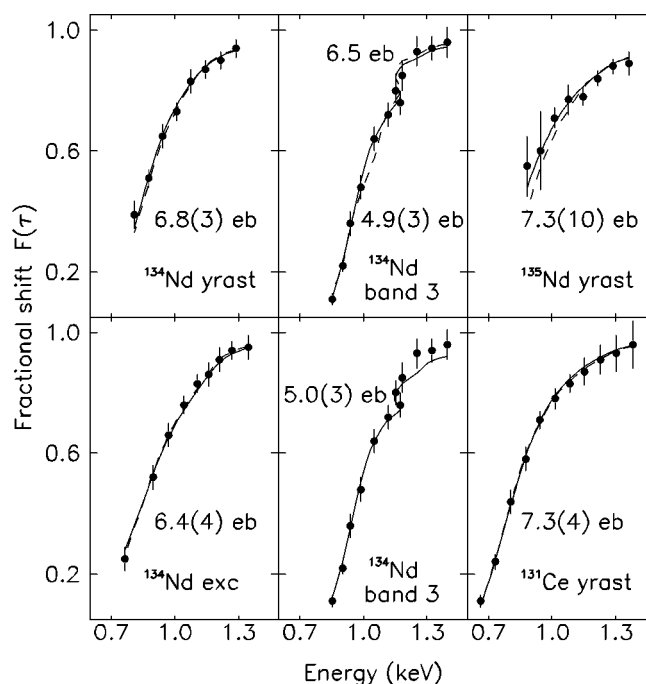


FIG. 2. Experimental (circles) and fitted (solid lines) $F(\tau)$ values for the high-spin bands in the $^{134,135}\text{Nd}$ and ^{131}Ce nuclei. The dynamic moments of inertia used to simulate the sidefeeding cascades are $J_{sf}^{(2)} = 50, 55, 45 \hbar^2 \text{ MeV}^{-1}$, for the bands of ^{134}Nd , ^{135}Nd , ^{131}Ce , respectively. The Q_0 values deduced from the best fits are indicated in each panel. The $F(\tau)$ values obtained by using the calculated quadrupole moments are drawn with dashed lines, which for the yrast and excited HD bands of ^{134}Nd and for ^{131}Ce are hardly distinguishable from the solid line fitting the experimental $F(\tau)$ values.

because in the band description used in the fitting procedure, we also included the known highest transitions in the bands which were observed in previous thin-target experiments with similar projectile-target combinations and beam energies, but not seen in the present thick-target data. The relatively slow sidefeeding of these transitions was an additional factor which led to fractional shifts smaller than 1 at the top of the bands. For the ^{131}Ce nucleus, which is populated after the evaporation of an α particle (and 3 neutrons), the reaction kinematics played a more important role. The momentum of the compound nucleus is modified by the evaporated massive α particle, which leads to a change of the velocity of the Ce residue. A Monte Carlo simulation has been used to correct for the reaction kinematics by taking into account the emission of α particles, leading to a value of the effective initial velocity for the ^{131}Ce recoils of $v_0/c=0.0192(2)$, which again is in good agreement with the Doppler shift of the highest observed transitions in the band.

The use of the DSAM method for relating the lifetime of a nuclear state to the recoil velocity has two serious limitations: (i) the stopping powers used to model the slowing down process are poorly known, and (ii) the lifetime of unresolved feedings introduce additional uncertainties in the final results. Since there are no experimental values for the slowing-down process of the ^{134}Nd ions in Pd and Au, we compared various parametrizations of the stopping powers [12–14] with the recent experimental values of Brandolini *et al.* [15] for ^{144}Nd ions in Pb, which show that the ‘‘best’’

TABLE I. The experimentally derived in-band (Q_0^{exp}) and sidefeeding (Q_{sf}) quadrupole moments, and the deduced quadrupole deformations β_2 (assuming no triaxiality) for high-spin bands in $^{134,135}\text{Nd}$ and $^{131,132}\text{Ce}$. The last column gives the range of variation of the calculated quadrupole moments (Q_0^{the}) for the observed states, whose spins are indicated in parenthesis.

Band	Q_0^{exp} (e b)	Q_{sf} (e b)	β_2	Q_0^{the} (e b)
^{134}Nd yrast HD	6.8(3)	6(1)	0.35(1)	7.4 (19)→5.9 (39)
^{134}Nd excited HD	6.4(4)	6(1)	0.33(2)	6.9 (18)→6.4 (40)
^{134}Nd band 3, lower part	4.9(3)	2.5(5)	0.26(2)	4.8 (18)→6.1 (26)
^{134}Nd band 3, upper part	~6.5	~6	~0.34	6.07 ^a (32→40)
^{134}Nd band 3, lower+upper	5.0(3)	4(1)	0.26(2)	
^{135}Nd HD	7.3(10)	3.0(5)	0.37(5)	6.4 (24.5)→5.5 (38.5)
^{131}Ce yrast HD	7.3(4)	6(1)	0.38(2)	7.5 (20.5)→6.7 (40.5)
^{132}Ce yrast HD ^b	7.4(3)		0.38(2)	8.0 (24)→6.6 (52)

^aAs we could not calculate the positive-parity configuration involving only one $i_{13/2}$ neutron, we estimated Q_0^{the} for the upper part of band 3 assuming that the contribution of one $i_{13/2}$ neutron is half of the calculated contribution of two $i_{13/2}$ neutrons $\{Q_0[(i_{13/2})^2]\}$ with respect to the configuration with zero $i_{13/2}$ neutrons ($\langle Q_0^L \rangle$), which is an average over the observed spin range in the lower part of band 3): $Q_0 = \langle Q_0^L \rangle + \frac{1}{2}\{Q_0[(i_{13/2})^2] - Q_0^L\} = (4.8 + 6.1)/2 + (6.69 - 5.45)/2 = 6.07$ e b.

^bFrom Ref. [6].

stopping powers are those of Northcliffe and Schilling [14]. Anyhow, regardless of which stopping powers are used, the relative quadrupole moments are the most significant result. The slowing down history of the recoiling nuclei was, therefore, calculated using the electronic stopping powers taken from the Northcliffe and Schilling tables [14], scaled according to the experimental values for ^4He ions as suggested by Sie *et al.* [16]. The nuclear contribution of the stopping power was treated using a Monte Carlo procedure according to the theory of Lindhard, Scharff, and Schiott [17] as parametrized by Winterbon [18]. The multiple scattering was treated in the Blaugrund approximation [19].

The spectra gated only on the high-lying transitions of the bands, where the sidefeeding contribution is much reduced, had a poor statistics and the extracted values of the centroid shifts were affected by errors too large to be of any practical use. Therefore, the centroid shifts were determined from double-gated spectra on all combinations of in-band transitions, in which the sidefeeding has full effect. The sidefeeding into each state was modeled by a single rotational cascade controlled by the dynamic moment of inertia $J_{(2)}^{sf}$ and the sidefeeding quadrupole moment Q_{sf} , both kept constant throughout the band. In all cases a cascade with only one transition was sufficient to reproduce the data, this being equivalent to the decay of a single unresolved state with an effective lifetime determined by all precursor states. The effective intensity of the sidefeeding has been determined by properly taking into account the procedure of generating the doubly gated spectra (gating on a transition of the band eliminates the sidefeeding for the states below this transition, but does not alter the sidefeeding of the states above it). The assumed spin independent parameters for the in-band and sidefeeding quadrupole moments (Q_0 and Q_{sf}) have been determined from a two-dimensional χ^2 minimization of the experimental $F(\tau)$ values. A constant dynamic moment of inertia for the sidefeeding of each band has been used, obtained from the average of the $J_{sf}^{(2)}$ values over the observed spin range.

The results of the fitting procedures for the bands of

$^{134,135}\text{Nd}$ and ^{131}Ce are shown in Fig. 2. The obtained in-band (Q_0^{exp}) and sidefeeding quadrupole moments (Q_{sf}), as well as the corresponding quadrupole deformations β_2 (assuming no triaxiality) are listed in Table I.

For ^{134}Nd , the quadrupole moments of band HD yrast, band HD excited and band 3 [8] have been obtained. The configurations of these three bands have been discussed in our previous works [2,8]. For the yrast HD band, involving one $\nu i_{13/2}$ intruder orbital, a quadrupole moment of 6.8(3) e b has been extracted. For the excited HD band, in which the lower part below the backbend involves one $\nu i_{13/2}$ orbital, whereas the higher part involves two $\nu i_{13/2}$ intruder orbitals [8], the extracted experimental quadrupole moment is $Q_0 = 6.4(4)$ e b. Band 3 of ^{134}Nd exhibits a bandcrossing at spin $\sim 30\hbar$, which marks the occupation of the first $\nu i_{13/2}$ intruder orbital [8] and therefore the data was fitted considering two distinct parts. For the upper part the fit gives a quadrupole moment of $Q_0 \sim 6.5$ e b. Since the number of experimental points is small (four) and they characterize the top part of the band which is quite insensitive to the quadrupole moment (the sensitive area is where the curvature of the fractional shift curve is large), this value has a large error (of the order of 20–30%) and therefore it must be considered with caution. For the lower part of the band, taking into account also the feeding by the upper part of the band with $Q_0 \sim 6.5$ e b, a quadrupole moment of 4.9(3) e b has been determined. In order to check this fitting procedure, the experimental fractional Doppler shifts of band 3 have also been fitted with a unique Q_0 value of 5.0(3) e b (see Fig. 2). The statistics of the present experiment does not allow one to distinguish firmly between the fits with constant or with two Q_0 values, even if the fit with an unique Q_0 passes below the highest experimental points (see Fig. 2). It has to be noted that for all three bands in ^{134}Nd the same sidefeeding ($Q_{sf} = 6$ e b and $J_{sf}^{(2)} = 50\hbar^2$ MeV $^{-1}$) was used. The present results for three high-spin bands of ^{134}Nd indicate that the measured quadrupole moments are not directly related to the number of occupied $\nu i_{13/2}$ intruder orbitals.

For the HD band of ^{135}Nd a quadrupole moment of $7.3(10) e b$ has been extracted. It must be noted, however, that a reasonable fit of the experimental $F(\tau)$ values is obtained with a much slower sidefeeding of $Q_{sf}=4.0(5) e b$. This result is in agreement with that reported by Diamond *et al.* [20], where a quadrupole moment of $Q_0=7.4(10) e b$ has been established with a sidefeeding of $Q_{sf}=3.5 e b$. This band has only one $\nu i_{13/2}$ intruder orbital occupied, and as expected, its quadrupole moment is close to that of the yrast HD in ^{134}Nd . The small quadrupole moment of the sidefeeding cascades can be an indication that at high spin, the near-yrast quasicontinuum is mainly composed of small-deformation (triaxial) bands. This is not unexpected, since the existence of high-spin triaxial bands in this mass region is well documented by recent results on ^{133}Ce [21] and ^{136}Nd [22].

For the yrast HD band of ^{131}Ce a quadrupole moment of $7.3(4) e b$ has been established, in good agreement with the $7.4(3) e b$ value of Clark *et al.* [6]. This value is much higher than the values obtained in Refs. [23] and [24], of $Q_0 \approx 6 e b$ and $5.5 e b$, respectively.

In order to elucidate the results of the present work, we performed extended cranked Strutinsky-type calculations, including quadrupole and monopole pairing correlations. The pairing field is calculated self-consistently and the Routhian is minimized with respect to the deformation parameters β_2 , β_4 , and γ at each step in frequency. For further details, see Ref. [25]. The expectation value of the quadrupole operators Q_{20} and Q_{22} are calculated using the intrinsic wave functions at the minimum of the total Routhian surface calculations.

A common feature revealed by the calculations for the HD bands with smooth behavior, i.e., where the number of occupied $\nu i_{13/2}$ orbitals (one or two) stays constant throughout the band, is a pronounced shrinking effect at high spins: the calculated quadrupole moments exhibit a decrease with spin of the order of 20% (see the fifth column of Table I). The reduction of β_2 as a function of rotational frequency has been explained [26] and discussed [27] for Yb isotopes in terms of the rotation-induced deoccupation of the anti-aligned high- j , low- Ω quasiparticle configurations (those in which the nucleons move in the opposite direction with respect to the nuclear rotation). The same effect exists also in the highly deformed Nd and Ce nuclei. It is caused by the Coriolis plus centrifugal forces and leads to the loss of anti-aligned high- j low- Ω orbits which have a strong polarizing effect on the nuclear shape, causing the nucleus to become less deformed and therefore resulting in a reduction of the Q_0 values.

In contrast with the decreasing values of the HD bands with smooth behavior, the calculated quadrupole moments of the bands where an additional $\nu i_{13/2}$ orbital is occupied at high spin (e.g., the excited HD band of ^{134}Nd) are nearly constant. This can be qualitatively understood through the compensation of the rotation-induced shrinking effect at high spins (which drives towards smaller deformation) by the polarizing force of the second $\nu i_{13/2}$ intruder orbital (which drives towards larger deformation). In such a simplified pic-

ture it is assumed that the most important factors which compete in determining the equilibrium deformation at high spin are the rotation-induced shrinking effect and the polarization by the $\nu i_{13/2}$ orbital. Note that calculations with the modified harmonic oscillator potential without pairing interaction yield quadrupole moments very similar to our calculations and a similar shrinking effect [7]. The statistics of the present data is not enough to allow for the measurement of the lifetime of each individual transition, and therefore this shrinking effect could not be determined. However, the fractional Doppler shifts obtained by using the calculated Q_0^{the} values give in general a good agreement (see the curves drawn with dashed lines in Fig. 1). Note that the experimental quadrupole moments have been deduced by fitting the $F(\tau)$ values with constant Q_0^{exp} .

The polarizing effect of the neutron $i_{13/2}$ intruder orbital can be studied at best in Nd and Ce isotopes, where the proton shell structure does not change over a rather wide region in rotational frequency [2]. Since the neutrons do not contribute to the charge-quadrupole moment, we deal with the pure shape-polarization effect of the $\nu i_{13/2}$ intruder orbital. However, the present calculations show that the polarizing effect of the $\nu i_{13/2}$ intruder orbital in the $A=130$ mass region is attenuated by the rotation-induced shrinking effect at high spin, which weakens the additivity relationship of quadrupole moments verified in the $A=150$ mass region [5]. In fact, neither in the excited HD band nor in band 3 of ^{134}Nd one observes a clear increase in deformation when the number of $\nu i_{13/2}$ intruder orbitals increases. In the case of band 3, the crossing is sharper than in the excited HD band, leading to a more localized distortion of the $F(\tau)$ curve. The rotation-induced shrinking manifesting over a broader spin range, is less effective in smoothing the crossing region between the configurations with zero and one $\nu i_{13/2}$ intruder orbitals. It is therefore easier (even if the statistics of the present experiment was not sufficient to give conclusive results) to determine individual Q_0 values for the regions below and above the crossing. The extracted quadrupole moment of $Q_0 \sim 6.5 e b$ for the higher part of band 3 (when fitted with different Q_0 values for the regions below and above the backbending) is very similar to that of the excited HD band of $Q_0=6.4(4) e b$. This is in agreement with the assigned configurations for the lower part of the excited HD band and for the higher part of band 3, which both involve a single $\nu i_{13/2}$ orbital.

In summary, lifetime measurements have been performed for three bands in ^{134}Nd , and for the yrast HD bands of ^{135}Nd and ^{131}Ce . The expected increase of the quadrupole moment of the excited HD band and band 3 of ^{134}Nd , which at high spin have an additional $\nu i_{13/2}$ orbital occupied, is smoothed by the reduction of the deformation due to the shrinking effect. The deduced fractional Doppler shifts for the five analyzed bands obtained using the calculated charge-quadrupole moments are in general good agreement with experiment, showing the adequacy of the cranked Strutinsky-type calculations of the deformation properties at high spins.

- [1] R. Wyss, J. Nyberg, A. Johnson, R. Bengtsson, W. Nazarewicz, *Phys. Lett. B* **215**, 211 (1988).
- [2] C. M. Petrache, S. Lunardi, D. Bazzacco, D. Bucurescu, G. de Angelis, C. Rossi Alvarez, C. A. Ur, and R. Wyss, *Phys. Lett. B* **353**, 307 (1994).
- [3] H. Savajols *et al.*, *Phys. Rev. Lett.* **76**, 4480 (1996).
- [4] D. Nisius *et al.*, *Phys. Lett. B* **392**, 18 (1997).
- [5] W. Satuła, Dobaczewski, J. Dudek, and W. Nazarewicz, *Phys. Rev. Lett.* **77**, 5182 (1996).
- [6] R. M. Clark *et al.*, *Phys. Rev. Lett.* **76**, 3510 (1996).
- [7] A. V. Afanasjev and I. Ragnarsson, *Nucl. Phys.* **A608**, 176 (1996).
- [8] C. M. Petrache *et al.*, *Phys. Lett. B* **387**, 31 (1996).
- [9] C. M. Petrache *et al.*, *Phys. Rev. Lett.* **76**, 239 (1996).
- [10] K. Hauschild *et al.*, *Phys. Rev. C* **52**, R2281 (1995).
- [11] T. K. Alexander and J. S. Foster, *Advances in Nuclear Physics*, edited by J. Negele and E. Vogt (Plenum, New York, 1979), Vol. 10, Chap. 3.
- [12] K. Braune, in *Heavy Ion Collision*, edited by R. Bock (North Holland, Amsterdam, 1983), Vol. 3, p. 279.
- [13] J. F. Ziegler, J. P. Biersack, and V. Littmark, *The Stopping Power and Range of Ions in Solid* (Pergamon, New York, 1985), Vol. 1.
- [14] L. C. Northcliffe and R. F. Schilling, *Nuclear Data, Sect. A* **7**, 256 (1970).
- [15] F. Brandolini, N. H. Medina, M. De Poli, P. Pavan, M. Wilhelm, A. Dewald, and G. Pascovici, *Nucl. Instrum. Methods Phys. Res. B* (in press).
- [16] S. H. Sie, D. Ward, J. S. Geiger, R. L. Graham, H. R. Andrews, *Nucl. Phys.* **A291**, 443 (1977).
- [17] J. Lindhard, M. Scharff, and H. E. Schiott, *Mat. Fys. Medd. K. Dan. Vidensk. Selsk.* **33**, 14 (1963).
- [18] K. B. Winterbon, Atomic Energy of Canada Limited Report, AECL-3914 (1968).
- [19] A. E. Blaugrund, *Nucl. Phys.* **88**, 501 (1966).
- [20] R. M. Diamond, C. W. Beausang, A. O. Macchiavelli, J. C. Bacelar, J. Burde, M. A. Deleplanque, J. E. Draper, C. Duyar, R. J. McDonald, and F. S. Stephens, *Phys. Rev. C* **41**, R1327 (1990).
- [21] K. Hauschild *et al.*, *Phys. Rev. C* **54**, 613 (1996).
- [22] C. M. Petrache *et al.*, *Phys. Lett. B* **373**, 275 (1996).
- [23] Y. He, M. L. Godfrey, I. Jenkins, A. J. Kirwan, P. J. Nolan, S. M. Mullins, R. Wadsworth, and D. J. G. Love, *J. Phys. G* **16**, 657 (1990).
- [24] S. M. Mullins, J. Nyberg, A. Maj, M. S. Metcalfe, P. J. Nolan, P. H. Regan, R. Wadsworth, and R. A. Wyss, *Phys. Lett. B* **312**, 272 (1993).
- [25] W. Satuła and R. Wyss, *Phys. Scr.* **T56**, 159 (1995).
- [26] J. D. Garrett *et al.*, in *Proceedings of the Conference on Contemporary Topics in Nuclear Structure Physics, Cocoyoc, Mexico*, edited by R. Casten, A. Frank, M. Moshinsky, and S. Pittel (World Scientific, Singapore, 1988), p. 699.
- [27] H. Xie, F. K. McGowan, C. Baktash, J. D. Garrett, J. H. Hamilton, N. R. Johnson, I. Y. Lee, J. C. Wells, R. Wyss, and C.-H. Yu, *Nucl. Phys.* **A599**, 560 (1996).